[10] B. Morris and M. Trivedi, "Learning, modeling, and classification of vehicle track patterns from live video," *IEEE Trans. Intell. Transp. Syst.*, vol. 9, no. 3, pp. 425–437, Sep. 2008.
[11] Z. Qin, "Method of vehicle classification based on video," in *Proc. IEEE/ASME Int. Conf. AIM*, 2008, pp. 162–164.
[12] N. Zeng and J. Crisman, "Vehicle matching using color," in *Proc. IEEE Conf. Intell. Transp. Syst.*, 1997, pp. 206–211.
[13] G. Kogut and M. Trivedi, "Maintaining the identity of multiple vehicles as they travel through a video network," in *Proc. IEEE Workshop Multi-Object Tracking*, 2001, pp. 29–34.
[14] A. MacCarley, *Video-Based Vehicle Signature Analysis and Tracking Phase 1: Verification of Concept Preliminary Testing*. Berkeley, CA: Univ. California, 1998.
[15] C. MacCarley, *Video-Based Vehicle Signature Analysis and Tracking System Phase 2: Algorithm Development and Preliminary Testing*. Berkeley, CA: Univ. California, 2001.
[16] J. Wright, A. Yang, A. Ganesh, S. Sastry, and Y. Ma, "Robust face recognition via sparse representation," *IEEE Trans. Pattern Anal. Mach. Intell.*, vol. 31, no. 2, pp. 210–227, Feb. 2008.
[17] L. Li, H. Su, E. Xing, and L. Fei-Fei, "Object bank: A high-level image representation for scene classification and semantic feature sparsification," in *Proc. NIPS*, Vancouver, BC, Canada, 2010.
[18] X. Mei and H. Ling, "Robust visual tracking and vehicle classification via sparse representation," *IEEE Trans. Pattern Anal. Mach. Intell.*, vol. 33, no. 11, pp. 2259–2272, Nov. 2011.
[19] J. Thiagarajan, K. Ramamurthy, and A. Spanias, "Sparse representations for pattern classification using learned dictionaries," in *Proc. 28th SGAI Int. Conf. Artif. Intell.*, 2008, pp. 33–45.
[20] A. Senior, A. Hampapur, Y. Tian, L. Brown, S. Pankanti, and R. Bolle, "Appearance models for occlusion handling," *Proc. Image Vis. Comput.*, vol. 24, no. 11, pp. 1233–1243, 2006.
[21] A. Verri and T. Poggio, "Motion field and optical flow: Qualitative properties," *IEEE Trans. Pattern Anal. Mach. Intell.*, vol. 11, no. 5, pp. 490–498, May 1989.
[22] J. Tropp and A. Gilbert, "Signal recovery from random measurements via orthogonal matching pursuit," *IEEE Trans. Inf. Theory*, vol. 53, no. 12, pp. 4655–4666, Dec. 2007.
[23] P. Zhao and B. Yu, "On model selection consistency of Lasso," *J. Mach. Learn. Res.*, vol. 7, pp. 2541–2563, Dec. 2006.
[24] F. Potra and S. Wright, "Interior-point methods," *J. Comput. Appl. Math.*, vol. 124, no. 1/2, pp. 281–302, 2000.
[25] T. Do, L. Gan, N. Nguyen, and T. Tran, "Sparsity adaptive matching pursuit algorithm for practical compressed sensing," in *Proc. 42nd Asilomar Conf. Signals, Syst. Comput.*, 2008, pp. 581–587.
[26] J. Tropp and S. Wright, "Computational methods for sparse solution of linear inverse problems," *Proc. IEEE*, vol. 98, no. 6, pp. 948–958, Jun. 2010.
[27] S. Ji, Y. Xue, and L. Carin, "Bayesian compressive sensing," *IEEE Trans. Signal Process.*, vol. 56, no. 6, pp. 2346–2356, Jun. 2008.
[28] M. Tipping, "Sparse Bayesian learning and the relevance vector machine," *Mach. Learn. Res.*, vol. 1, pp. 211–244, Sep. 2001.
[29] A. Papoulis, S. Pillai, and S. Unnikrishna, *Probability, Random Variables, and Stochastic Processes*. New York: McGraw-Hill, 2002.
[30] J. Bernado and A. Smith, *Bayesian Theory*. New York: Wiley, 1994.

Estimation of Lane Marker Parameters With High Correlation to Steering Signal

A. Demčenko, M. Tamošiūnaitė, A. Vidugirienė, and L. Jakevičius

***Abstract*—This paper considers the design and analysis of lane marker parameters in 2-D images. Five different parameters, which have high correlation to the steering angle of a vehicle, are proposed, and their correspondence to the steering signal is analyzed. The parameters are based on the position, angle, area, and curvature of the lane marker and have not been reported in the literature before, except the curvature. A new derivative-free method is proposed for curvature estimation. The stability of the proposed parameters is analyzed with respect to the look-ahead distance. Possible application of the parameters for overtaking detection is presented. This paper is performed using signals from real country road driving.**

***Index Terms*—Driver's assistance, human-like driving, lane marker, steering signal.**

I. Introduction

The drivers' behavior, which involves braking, acceleration/deceleration, and steering, is complex and individual [1]–[4]. Individualized assistance in some isolated driver's actions, e.g., steering or braking, is possible, and such systems are under development or even integrated into modern vehicles [5], [6]. However, much more of the current autonomous driving technologies still stick with standard approaches where the control provided by the system is clearly based on physical laws and does not consider the driver's individuality [7]–[10]. If such principles are applied for human assistance, the systems may interpret the driver's behavior in a wrong way and produce a false control or warning signal. Thus, the design of a reliable driver's assistance system (DAS) for the individual driver's behavior prediction and assistance at different driving conditions is a challenge and is an important direction in the future development of intelligent DAS.

Lane markers on a road can provide reliable and useful information for DAS [11]. Many lane keeping systems usually involve vision systems that perform lane marker detection, recognition, and tracking [1], [12], [13]. However, direct use of the lane marker shape for the vehicle's control assistance is complicated; therefore, it is desirable to parameterize the lane markers by features [14]. In existing literature on driving assistance, mainly a curvature parameter is exploited [14]–[16], but a more general analysis of the parameters of a 2-D visual scene was never performed. The parameters in the car's coordinate system, like lateral offset of the lane marker and orientation of the lane

Manuscript received June 8, 2010; revised January 31, 2011, July 11, 2011 and November 11, 2011; accepted December 3, 2011. Date of publication January 5, 2012; date of current version May 30, 2012. This work was supported in part by the European Commission project "Learning to Emulate Perception—Action Cycles in a Driving School Scenario" (DRIVSCO), FP6-IST-FET, under Contract 016276-2. The Associate Editor for this paper was N. Papanikolopoulos.

A. Demčenko was with the Department of Applied Informatics, Vytautas Magnus University, Kaunas 44404, Lithuania. He is now with the Faculty of Engineering Technology, University of Twente, 7500 Enschede, The Netherlands (e-mail: andriejus.demcenko@gmail.com).

M. Tamošiūnaitė and A. Vidugirienė are with the Department of System Analysis, Vytautas Magnus University, Kaunas 44404, Lithuania (e-mail: m.tamosiunaite@if.vdu.lt; ausrine@gmail.com).

L. Jakevičius is with the Department of Physics, Kaunas University of Technology, Kaunas 51368, Lithuania (e-mail: leonas.jakevicius@ktu.lt).

Color versions of one or more of the figures in this paper are available online at http://ieeexplore.ieee.org.

Digital Object Identifier 10.1109/TITS.2011.2179535

marker, have been suggested for lateral control (steering) [7], [17], but a comparison with the 2-D image parameters has not been provided in the mentioned studies. In driver's behavior literature, a tangent point is hypothesized to govern the steering on a curved road [18], [19], but the tangent point rather defines a control strategy, and it is not a parameter of the 2-D scene that correlates to the steering signal on its own.

The objective of this paper is to design and analyze lane marker parameters derived from 2-D images with high correlation to the vehicle's steering signal. Four new parameters and a new algorithm for curvature calculation (the fifth parameter analyzed in this paper) are introduced. The introduced parameters are estimated from visual data recorded during usual driving on country roads. The stability of the parameters is investigated with respect to look-ahead distance (i.e., height coordinate of the image where the parameters are estimated). The estimation results are compared with the steering signal evaluating cross-correlation coefficients between the signals. A possible application of the parameters for steering signal prediction and overtaking action detection is presented.

II. Data

Data were collected on country roads in Germany. The driving action sequences were simultaneously recorded with the traffic scenario. The analyzed records were performed in the years 2006–2008 by different drivers on different routes.

The driving data analyzed here consist of two different parts: the first part is provided by a CAN bus, and the second part is provided by a video camera installed in the car. The CAN bus data include the driver's behavior action recordings (steering, braking, acceleration, etc.) and information related to the vehicle (velocity, position on the lane, etc.). The video camera data were captured at 20 or 25 Hz and had image dimensions of 1280×1024 pixels.

A right-side lane marker is usually best visible on the country road camera images, and it can most readily be extracted. In this paper, the right-side lane marker data (x and y coordinates in pixels) were extracted from the captured images using an algorithm based on an edge detection method [20].

III. Parameters

Five different lane marker parameters are proposed and analyzed here: 1) x coordinate variation x_v measured at the fixed y coordinate; 2) angle α between lane marker and horizontal line at fixed y coordinate; 3) area s estimated from a lane marker curve segment in a frame; 4) maximum m of the lane marker x and y coordinate ratio in a frame; and 5) curvature c of the lane marker (including a new algorithm for curvature evaluation). All the five parameters are further presented in more detail.

A. Variation of x Coordinate x_v

Depending on the curvature of the road, the upper part of the lane marker appears more to the right (for the right curve) or more to the left (for the left curve) in the camera image. The parameter "variation of x coordinate" x_v is based on this lane marker position variability. Fig. 1 presents the coordinate system and illustrates a case when a segment of the country road is curved first to the right and in far distance to the left. The red curve is the estimated lane marker on the road. The upper horizontal line indicated in Fig. 1(a) is used for the estimation of the parameter x_v, and its coordinates are defined *a priori*. Above the horizontal line, the lane marker is not informative for an immediate driver's steering action (in the given example: negotiation of the right curve). Going down from the horizontal line, the x position of the lane marker becomes less variable with the road curvature. Accordingly,

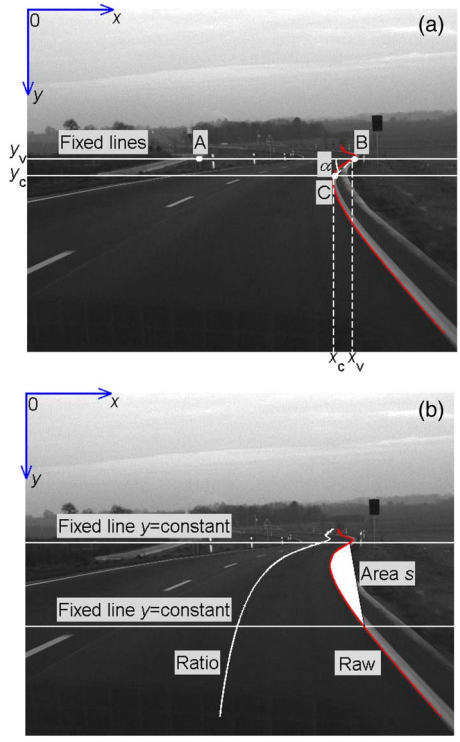

Fig. 1. Estimation of the lane marker parameters. (a) Variation x_v and angle α. (b) Area s and illustration of raw lane marker (red curve) and scaled lane marker (x/y, white curve). Red curve is the estimated lane marker; horizontal lines are the additional lines for the estimation of lane marker parameters. The proportions are true except for ratio x/y.

there is an interval along the image height coordinate y (which roughly corresponds to image depth in 3-D or look-ahead), where the position of the lane marker will correlate with the upcoming curvature and with the upcoming steering action.

The parameter is measured at some predefined value of y coordinate. In our setup, the lane markers can be extracted stably up to $y = 450$ pixels (this value corresponded to 33 m in a look-ahead distance). The parameter stability analysis presented later in this paper confirms that a wide interval of the y (look-ahead) values may be applied for parameter construction.

B. Angle α

A right lane marker on a camera image most of the time is tilted to the left due to perspective effects. However, the degree of tilt varies with the road curvature, and on more pronounced right curves, the lane marker tilts to the right in some parts of the image, as shown in Fig. 1. An angle α of the lane marker to the horizontal line can be considered as the feature to reflect this left-right tilt of the lane marker and, consequently, left and right steering actions. The angle is estimated by applying the law of cosines for the triangle ABC using coordinate values of the lane marker x_c, y_c and x_v, y_v, as shown in Fig. 1(a).

C. Area s

A lane marker extracted from visual data may contain noise. To cope with the small-scale noise components on the extracted lane marker, an area-based parameter is introduced. Two points are chosen to denote the beginning and end of the lane marker segment. By connecting those two points by a straight line, it is possible to calculate the area inside the loop [Fig. 1(b)]. The area increases as the road curvature increases and vice versa.

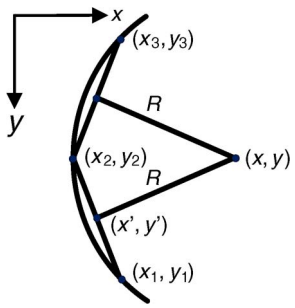

Fig. 2. Geometry for curvature estimation. The first vector involved in curvature estimation is given by the coordinates (x_1, y_1) and (x_2, y_2), and the second vector is denoted by the coordinates (x_2, y_2) and (x_3, y_3).

D. Maximum Ratio m

Let the lane marker coordinate x and y ratio be denoted $r_{x/y}$: The ratio and the raw lane marker are presented in Fig. 1(b). The scaling of the x coordinates by the y coordinate acts in the direction of the perspective restoration [21]. The maximum value of the ratio along the lane marker here is called m and considered as a parameter for steering prediction. Thus, parameters m and x_v are estimated in different coordinate systems. The m parameter is calculated in the coordinates proportional to the 3-D world scene, and x_v is calculated in the 2-D image area coordinates.

E. Curvature

Curvature is one of the most frequently used parameters for the characterization of a lane marker on a road [14]–[16]. Usually, curvature, given by a planar curve $C = (x(t), y(t))$, is estimated from the following generalized expression [22]:

$$c = \left(x'(t)y''(t) - x''(t)y'(t)\right) / \left(x'(t)^2 + y'(t)^2\right)^{3/2} \quad (1)$$

where x' and x'' denote the first- and second-order derivatives of the curve parameters, respectively. As derivatives are employed, the estimation of the curvature is numerically unstable. To overcome this numerical instability, the derivative-free method for curvature estimation is proposed below.

Two vectors are perpendicular when their scalar product is 0. In this paper, the two vectors are given by the beginning and end points: (x_1, y_1) and (x_2, y_2), (x', y'') and (x, y). The geometry is shown in Fig. 2.

The middle point, denoted by the coordinates (x', y') (Fig. 2), of the first vector is given by

$$x' = (x_1 + x_2)/2, \quad y' = (y_1 + y_2)/2. \quad (2)$$

For two perpendicular vectors, given by the end coordinates (x_1, y_1) and (x_2, y_2), and (x', y') and (x, y), the product can be written as

$$(x_2 - x_1)(x - x') + (y_2 - y_1)(y - y') = 0. \quad (3)$$

The system of linear equations for two spans, given by the two vectors (Fig. 2), can be written as

$$\begin{cases} y = (y_2+y_1)/2 + (x_2-x_1)/(y_1-y_2)\,(x-(x_2+x_1)/2) \\ y = (y_3+y_2)/2 + (x_3-x_2)/(y_2-y_3)\,(x-(x_3+x_2)/2)\,. \end{cases} \quad (4)$$

Assuming that $y_2 - y_1 = y_3 - y_2$ and then denoting the difference as Δy, (4) is solved for the coordinate x as

$$x = \left(\left(x_2^2 - x_1^2\right) - \left(x_3^2 - x_2^2\right) - 2\Delta y\right) / \left(2\left[(x_2 - x_1) - (x_3 - x_2)\right]\right). \quad (5)$$

To estimate the curve radius R (Fig. 2), it is necessary to evaluate the y coordinate. The y coordinate can be calculated using (4) when x is known from (5). When y_1, y_2, and y_3 are fixed, for a parameter that is proportional to the curvature, it is enough to estimate the x coordinate. In this case, the pseudo-curvature c can be written as

$$c = 1/x. \quad (6)$$

Finally, in the curvature analysis, a variable x is replaced by the ratio x/y, which acts as perspective restoration, as mentioned in Section III-D.

TABLE I
ESTIMATED CROSS-CORRELATION COEFFICIENTS BETWEEN THE PRESENTED PARAMETERS AND THE VEHICLE'S STEERING SIGNALS

No	Year	N_S	ρ_x	ρ_α	ρ_S	ρ_m	ρ_C	$\theta_{\min}$ / $\theta_{\max}$, deg.
1	2006	1600	0.92	0.76	0.85	0.91	0.89	-21 / 21
2			0.94	0.95	0.91	0.90	0.93	-17.5 / 14
3			0.96	0.93	0.90	0.90	0.85	-19.25 / 101.5
4			0.87	0.75	0.70	0.85	0.76	-42 / 101.5
5		1106	0.85	0.56	0.68	0.85	0.77	-42 / 29.75
6		1600	0.93	0.81	0.86	0.93	0.91	-21 / 15.75
7			0.86	0.66	0.93	0.92	0.86	-15.75 / 15.75
8			0.74	0.59	0.78	0.78	0.38	-21 /12.25
9			0.98	0.94	0.89	0.95	0.92	-43.75 / 108.5
10		1292	0.95	0.86	0.93	0.95	0.92	-47.25 / 29.75
11	2007	897	0.98	0.87	0.96	0.96	0.97	-31.5 / 15.75
12		1600	0.97	0.90	0.97	0.98	0.97	-22.75 / 19.25
13		1251	0.93	0.85	0.96	0.92	0.96	-22.75 / 21
14		1291	0.83	0.83	0.90	0.79	0.91	-17.5 / 8.75
15		1600	0.92	0.78	0.84	0.93	0.85	-40.25 / 22.75
16			0.98	0.89	0.97	0.94	0.98	-35 / 44
17		1366	0.92	0.78	0.86	0.87	0.85	-12.75 / 7.5
18	2008	1361	0.93	0.80	0.91	0.84	0.89	-22 / 10.75
19		851	0.93	0.92	0.92	0.93	0.93	-21 /17.5
20		1020	0.97	0.94	0.88	0.95	0.92	-36.75 / 33.25
M / std		-	0.93 / 0.06	0.84 / 0.11	0.90 / 0.08	0.92 / 0.06	0.91 / 0.13	-

IV. RESULTS

To determine the quality of the presented lane marker parameters, cross-correlation coefficients are calculated between the parameters and the steering signal for 20 driving data sets. The results are listed in Table I. In Table I, the following notation is introduced: N_s is the number of samples in the data set, and $\theta_{\min}$ and $\theta_{\max}$ are the minimum and maximum amplitudes of the steering signal in degrees, respectively. ρ_x, ρ_α, ρ_s, ρ_m, and ρ_c are the cross-correlation coefficients between the vehicle's steering signal and the lane marker parameters: the coordinate variation x_v, the angle α, the area s, the maximum ratio m, and the curvature c, respectively.

The cross-correlation coefficients listed in Table I are evaluated using the following initial conditions: the x_v parameter is estimated by tracing the lane marker data at $y = 500$ pixels, and the angle α is calculated when two points in the lane marker data are estimated at $y_v = 500$ pixels and at $y_c = 550$ pixels [see Fig. 1(a)]. The area s is estimated for a lane marker segment between $y = 500$ and 700 pixels, respectively [Fig. 1(b)]. The maximum ratio m is calculated by limiting the lane marker from 500 pixels to the end, i.e., rejecting the lane marker part below 500 pixels. The curvature c is calculated by applying (5) and (6) with $y_1 = 700$ pixels, $y_2 = 600$ pixels, and $y_3 = 500$ pixels (Fig. 2).

The results listed in Table I show that in most cases, the correlation is above 0.9, but in some cases, the cross-correlation coefficients are significantly lower. A major part of these low correlation values is caused by a missing lane marker due to side streets or lane marker deterioration. As this paper is not concentrating on lane marker extraction techniques, no specific processing for special situations like

vanishing road markers is employed. Instead, gaps in the parameter vectors are interpolated by cubic splines.

Summarizing the results listed in Table I, correlations of up to $\rho = 0.98$ can be achieved for both lane marker curvature c and x coordinate variation x_v. Estimated medians (see the last row in Table I) show that if one wants to achieve the highest correlation with the steering signal, one should use x coordinate variation parameter x_v. The lowest correlation can be expected between angle α and the steering signal. However, the medians M and standard deviations of the cross-correlation coefficients prove good correlation with low variance in the obtained correlation values between the steering signal and all the investigated parameters.

V. Stability of Parameters

The stability of the lane marker parameters is analyzed with respect to the look-ahead distance (in the image appearing as a vertical shift of the area where analysis is performed). The stability is evaluated by shifting the horizontal lines used for parameter estimation (see Fig. 1) up and down the image and by changing the distance between the lines (when more than one line is used for parameter estimation).

Fig. 3 shows the estimated cross-correlation coefficients between the steering signal and the lane marker parameters. The illustrations are presented for data set No. 16 listed in Table I. Fig. 3(a) shows how cross-correlation coefficients depend on the look-ahead distance when the lane marker parameter x_v is investigated. The horizontal axis y corresponds to the look-ahead distance. The result shows that the cross-correlation coefficient goes down with the reduction of the look-ahead distance. However, in a relatively wide range, i.e., $450 < y < 527$ pixels, the cross-correlation coefficient above 0.95 is obtained.

The estimated cross-correlation coefficients between the lane marker parameter α and the steering signal are presented in Fig. 3(b). The solid curve shows how the correlation coefficient depends on the look-ahead distance. The curve is obtained using the following parameters: the upper line [see Fig. 1(a)] at $y = 450$ pixels and the lower line at $y = 500$ pixels. The correlation coefficients are estimated in the range $450 \leq y \leq 600$ pixels for the upper line position. After that, the upper line is placed at $y = 506$ pixels, i.e., where a maximum of the cross-correlation coefficient is obtained. The lower line is placed one pixel below, i.e., at $y = 507$ pixels. The cross-correlation coefficients are estimated by shifting down the position of the lower line and thus increasing the width of the interval in which the angle is estimated. The resulting cross-correlation coefficients are presented in Fig. 3(b) by the dotted curve. The results show [Fig. 3(b)] that the parameter angle α strongly depends on the look-ahead distance (solid curve) and has a low dependence on the lane marker segment width in which the parameter is estimated (dotted curve).

Cross-correlation coefficients between the lane marker parameter area s and the vehicle's steering signal are presented in Fig. 3(c). The solid curve shows the cross-correlation coefficient dependence on the look-ahead distance, and the dotted curve shows the cross-correlation coefficient dependence on the employed lane marker segment width. As initial conditions, the upper and lower lines [see Fig. 1(b)] are at $y = 450$ pixels and $y = 650$ pixels, respectively. In the second part of the experiment, the upper line is at $y = 495$ pixels, and the lower line passes the range $496 \leq y \leq 696$ pixels. The results [see Fig. 3(c)] show that the area s does not change much with the change of the look-ahead distance (range $480 \leq y \leq 552$), but it has low correlation to the steering signal when the look-ahead distance is below $y = 480$ pixels. In addition, one can see that the cross-correlation coefficient becomes low when the look-ahead distance is above $y = 558$ pixels. The dotted curve [Fig. 3(c)] shows that a narrow window (approximately up to 50 pixels of the lane marker segment) results in relatively low correlation between the area s and the steering signal, but the wider lane marker window (more than 50 pixels) increases the correlation that grows with the window size.

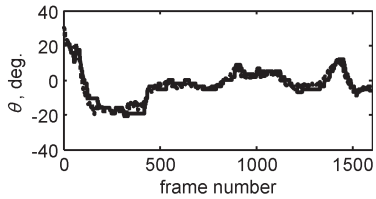

Fig. 4. Steering signals: true (solid curve) and predicted (dotted curve). The steering signal prediction mean squared error is 2.83%.

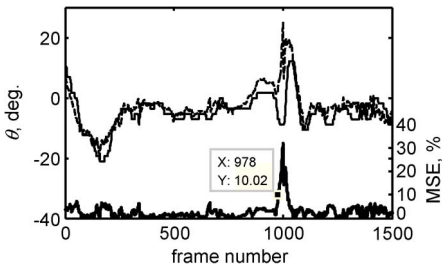

Fig. 5. Illustration of overtaking action: predicted steering signal (dashed curve) and true signal (solid curve); below mean squared error of the predicted steering signal.

The cross-correlation coefficients between the lane marker parameter m and the steering signal when the maximum look-ahead distance varies are presented in Fig. 3(d). The results show that evaluation of the parameter m is unstable in the range $450 \leq y \leq 485$ pixels, but beyond 485 pixels, the correlation becomes stable. It can be observed that decreasing the look-ahead distance reduces the cross-correlation coefficient between the parameter m and the steering signal.

The investigated cross-correlation coefficients between the steering signal and the lane marker curvature c are presented in Fig. 3(e). The following initial conditions are applied: three points (see Fig. 2) are placed at $y_1 = 450$, $y_2 = 550$, and $y_3 = 650$ pixels. The cross-correlation coefficient between the curvature and the steering signal is estimated [solid curve, Fig. 3(e)], simultaneously shifting all the three points. The results show that the correlation decreases (due to unstable curvature estimation) when the lowest point (initial position $y = 650$ pixels) approaches 760 pixels. The dotted line [see Fig. 3(e)] shows the cross-correlation coefficient when the middle point (x_2, y_2; Fig. 2) coordinate y_2 is varied. In this case, the initial conditions are as follows: The uppermost and lowest points are fixed at $y = 511$ and $y = 711$ pixels. The middle point coordinate varies in the range $512 \leq y_2 \leq 710$ pixels. The results show that the position of the coordinate y_2 between y_1 and y_3 has very little influence on the correlation between the curvature c and the steering signal.

VI. Applications

Here, we show how the proposed lane marker parameters can be applied for the detection of an overtaking action. A neural network, specifically the extreme learning machine [23], is used for steering signal prediction. A hidden layer has four neurons and the sigmoid transfer function. Training is performed using signal Nos. 2–5 (see Table I), and signal No. 1 is used for testing.

An illustration of the predicted signal is presented in Fig. 4 (prediction error 2.83%). The steering signal prediction accuracies using different lane marker combinations were presented in our previous work [24].

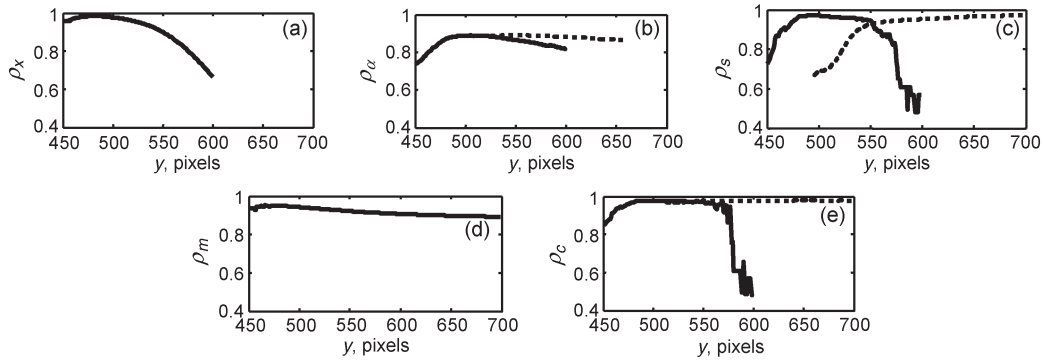

Fig. 3. Cross-correlation coefficient between the steering signal and the lane marker parameters. (a) x_v parameter correlation to steering signal for the interval of y values. (b) Angle α correlation to the steering signal for the interval of y values when the width of evaluation window is 50 pixels (solid curve) and angle α correlation to the steering signal when $y = 507$ and the width of evaluation window varies. (c) Area s correlation to the steering signal for the interval of y values when the evaluation window is 200 pixels (solid curve) and area s correlation to the steering signal when $y = 495$ and the width of evaluation window varies (dotted curve). (d) Maximum ratio m correlation to the steering signal for the interval of y values. (e) Curvature c correlation to the steering signal for the interval of y values when the evaluation window is 200 pixels and point y_2 (Fig. 2) is in the middle between points y_1 and y_3 (solid curve) and correlation to the steering signal when the y_2 coordinate varies (dotted curve).

Fig. 5 shows the predicted steering signal and the prediction error during overtaking action of a bicyclist. This overtaking action made it possible to analyze the lane marker parameters without additional interpolation of the parameters because the estimation of the lane marker on the road was not strongly distorted or hidden by the bicyclist. The presented results show that the prediction error increases rapidly during the overtaking action. The error level above 10% of the mean square error, which here will be considered as a threshold level, coincides well with the beginning of the overtaking action (starting at frame number 970). The time delay between the beginning of the overtaking action and the steering signal prediction error overcoming the threshold is 0.32 s.

VII. Discussion

Four new lane marker parameters, i.e., the x coordinate variation x_v estimated at the fixed y coordinate, the angle α between the lane marker and the horizontal line at a fixed y coordinate, the area s estimated from a lane marker curve segment, and the maximum m of the lane marker x and y coordinate ratio in a frame, are introduced. The fifth parameter analyzed in this paper is the curvature c of the lane marker, which is long known in autonomous driving literature, but here we propose a new method for curvature estimation. All five parameters are estimated from monocamera images and have high correlation to the vehicle's steering signal. The highest correlation to the steering signal is obtained using parameters x_v (mean correlation 0.93) and m (mean correlation 0.92), and the lowest correlation is obtained using angle α (mean correlation to the steering signal 0.84). It is shown that the proposed parameters are stable with respect to the change of look-ahead distance in relatively wide intervals, which would guarantee parameter stability with respect to small shifts of coordinate frame, which may happen due to different placement of cameras in different vehicles. The best stability with respect to look-ahead distance is achieved for parameters x_v, s, and c. Consequently, the only parameter that has slightly worse properties is the angle α. Any of the remaining four parameters could be used for steering angle prediction on its own, or all parameters may be used together (although correlated in between) to compensate for estimation noise.

Recent methods enable the reconstruction of the real road (bird's eye view) geometry [25], but the results presented in this paper indicate that already features from 2-D image analysis are sufficient to predict the steering signal with high accuracy. One should agree that reconstruction of the real road geometry makes it easier to reason about current traffic situation in human-like terms (e.g., the vehicle is 2 m away from the right lane marker and turned toward the lane marker at the angle of 20°), which our features do not support. Alternatively, this knowledge in the proposed features is implicit and allows making predictions using black-box models like neural networks, as would be discussed further.

As the presented features have correlation to the steering signal up to 0.98, only the few remaining percentages in accuracy are left for improvement using more features, or more advanced features, e.g., adding 3-D information, like slope or bank angle (superelevation) of the road [26]. One can expect that slope information would be much more important on hilly roads, whereas the data that were analyzed here were obtained in flat surroundings. Superelevation would make a difference in the circumstances where the roads are less standardized but apparently does not make a big difference for driving on highly standardized German roads.

It was shown that employing presented lane marker parameters makes it possible to achieve steering signal prediction error smaller than 3%. Application of the lane marker parameters to detect the overtaking maneuver through monitoring prediction error was presented. Detection of the driver's action was done with respect to the driver's "normal" driving, where a neural network had learned the normal driving pattern of this specific driver before. As suggested by the given application example, through predicting the driver's behavior and analyzing inconsistencies, adaptive DAS that takes into account human-like driving can be developed.

It was reported [16] that an autonomous vehicle drove in a more stable manner than the human driver. That is true because all conventional driving systems try to keep a vehicle exactly at the position on a road that is considered optimal. However, a human driver has his individual driving style and experience; therefore, a mismatch between the human driver and autonomous driving can cause an incorrect interpretation of the driving situation for DAS.

For the overtaking action detection presented here, the steering signal prediction error rapidly grows with the beginning of the overtaking action, and thus, the action can be detected by analyzing the error signal (e.g., introducing a threshold). The same strategy can be used for lane change detection and for the detection of incorrect or unsafe driving supplemented by triggering of the warning message for the driver in case of need [27].

A DAS that uses a visual system for the estimation of lane marker parameters on a road may fail when the lane marker is missing or illumination is unfavorable. However, a lane marker failure can be

compensated by GPS and map data [12], [28], [29] or vehicle to vehicle and vehicle to infrastructure communications [30]. Even when using other sources than vision to obtain lane information, some of the designed features (or their analogs for the nonvision scene) can be advantageously used for steering action prediction.

REFERENCES

[1] S.-J. Wu, H.-H. Chiang, J.-W. Perng, C.-J. Chen, B.-F. Wu, and T.-T. Lee, "The heterogeneous systems integration design and implementation for lane keeping on a vehicle," *IEEE Trans. Intell. Transp. Syst.*, vol. 9, no. 2, pp. 246–263, Jun. 2008.

[2] N. Kuge, T. Yamamura, O. Shimoyama, and A. Liu, "A driver behavior recognition method based on a driver model framework," *SAE Trans.*, vol. 109, no. 6, pp. 469–476, 2000.

[3] W. Enkelmann, "Video-based driver assistance-from basic functions to applications," *Int. J. Comput. Vis.*, vol. 45, no. 3, pp. 201–221, Dec. 2001.

[4] L. Fletcher, G. Loy, N. Barnes, and A. Zelinsky, "Correlating driver gaze with the road scene for driver assistance systems," *Robot. Autonom. Syst.*, vol. 52, no. 1, pp. 71–84, May 2005.

[5] K. Maček, R. Philippsen, and R. Siegwart, "Path following for autonomous vehicle navigation based on kinodynamic control," *J. Comput. Inf. Technol.*, vol. 17, no. 1, pp. 17–26, 2009.

[6] S. Vitabile, S. Bono, and F. Sorbello, "An embedded real-time lane-keeper for automatic vehicle driving," in *Proc. Int. Conf. CISIS*, 2008, pp. 279–285.

[7] S. Mammar, S. Glaser, and M. Netto, "Time to line crossing for lane departure avoidance: A theoretical study and an experimental setting," *IEEE Trans. Intell. Transp. Syst.*, vol. 7, no. 2, pp. 226–241, Jun. 2006.

[8] M. Schulze, T. Mäkinen, J. Irion, M. Flament, and T. Kessel, IP PReVENT Final Report, 2008. [Online]. Available: http://www.prevent-ip.org/download/deliverables/IP_Level/PR-04000-IPD-080222-v15_PReVENT_Final_Report_Amendments%206%20May%202008.pdf

[9] L. Fu, A. Yazici, and Ü. Özgüner, "Route planning for OSU-ACT autonomous vehicle in DARPA urban challenge," in *Proc. IEEE Intell. Veh. Symp.*, Eindhoven, The Netherlands, 2008, pp. 781–786.

[10] J. Ziegler, M. Werling, and J. Schröder, "Navigating car-like robots in unstructured environments using an obstacle sensitive cost function," in *Proc. IEEE Intelligent Vehicles Symposium*, Eindhoven, The Netherlands, 2008, pp. 787–791.

[11] J. C. McCall and M. M. Trivedi, "Video-based lane estimation and tracking for driver assistance: Survey, system, and evaluation," *IEEE Trans. Intell. Transp. Syst.*, vol. 7, no. 1, pp. 20–37, Mar. 2006.

[12] J. Valldorf and W. Gessner, *Advanced Microsystems for Automotive Applications*. New York: Springer-Verlag, 2006.

[13] H. G. Jung, Y. H. Lee, H. J. Kang, and J. Kim, "Sensor fusion-based lane detection for LKS+ACC system," *Int. J. Autom. Technol.*, vol. 10, no. 2, pp. 219–228, Apr. 2009.

[14] K. A. Redmill, S. Upadhya, A. Krishnamurthy, and Ü. Özgüner, "A lane tracking system for intelligent vehicle applications," in *Proc. IEEE Intell. Transp. Syst. Conf.*, Oakland, CA, 2001, pp. 273–279.

[15] G. Xiong, P. Zhou, S. Zhou, X. Zhao, H. Zhang, J. Gong, and H. Chen, "Autonomous driving of intelligent vehicle BIT in 2009 future challenge of China," in *Proc. IEEE Intell. Veh. Symp.*, San Diego, CA, 2010, pp. 1049–1053.

[16] K. B. Lee and M. H. Han, "Lane-following method for high speed autonomous vehicles," *Int. J. Autom. Technol.*, vol. 9, no. 5, pp. 607–613, Oct. 2008.

[17] D. Koller, Q.-T. Luong, and J. Malik, "Using binocular stereopsis for vision-based vehicle control," in *Proc. IEEE Intell. Veh. Symp.*, Paris, France, 1994, pp. 237–242.

[18] M. F. Land and D. N. Lee, "Where we look when we steer," *Nature*, vol. 369, no. 6483, pp. 742–744, Jun. 1994.

[19] F. I. Kandil, A. Rotter, and M. Lappe, "Driving is smoother and more stable when using the tangent point," *J. Vis.*, vol. 9, no. 1, pp. 1–11, Jan. 2009.

[20] A. Vidugirienė, A. Demčenko, and M. Tamošiūnaitė, "Extraction and investigation of lane marker parameters for steering signal prediction," in *Proc. 12th Int. Conf. Transport Means*, Kaunas, Lithuania, 2008, pp. 143–146.

[21] B. Cyganek and J. P. Siebert, *An Introduction to 3D Computer Vision Techniques and Algorithms*. Chippenham, U.K.: Willey, 2009.

[22] D. Marsh, *Applied Geometry for Computer Graphics and CAD*. New York: Springer-Verlag, 2005.

[23] G.-B. Huang, Q.-Y. Zhu, and C.-K. Siew, "Extreme learning machine: Theory and applications," *Neurocomputing*, vol. 70, no. 1–3, pp. 489–501, Dec. 2006.

[24] A. Demčenko, M. Tamošiūnaitė, A. Vidugirienė, and L. Jakevičius, "Lane marker parameters for vehicle's steering signal prediction," *WSEAS Trans. Syst.*, vol. 8, no. 2, pp. 251–260, Feb. 2009.

[25] Y. Sebsadji, N. Benmansour, S. Glaser, S. Mammar, D. Aubert, and D. Gruyer, "3D Estimation of road cartography using vehicle localization and observers," in *Proc. 10th Int. Conf. Control, Autom. Robot. Vis.*, Hanoi, Vietnam, 2008, pp. 451–457.

[26] S. Glaser, S. Mammar, and C. Sentouh, "Integrated driver-vehicle-infrastructure road departure warning unit," *IEEE Trans. Veh. Technol.*, vol. 59, no. 6, pp. 2757–2771, Jul. 2010.

[27] P. Angkititrakul, R. Terashima, and T. Wakita, "On the use of stochastic driver behavior model in lane departure warning," *IEEE Trans. Intell. Transp. Syst.*, vol. 12, no. 1, pp. 174–183, Mar. 2011.

[28] D. Bétaille and R. Toledo-Moreo, "Creating enhanced maps for lane-level vehicle navigation," *IEEE Trans. Intell. Transp. Syst.*, vol. 11, no. 4, pp. 786–798, Dec. 2010.

[29] J. M. Alvarez, F. Lumbreras, T. Gevers, and A. M. López, "Geographic information for vision-based road detection," in *Proc. IEEE Intell. Veh. Symp.*, San Diego, CA, 2010, pp. 621–626.

[30] J. Santa, A. F. Gómez-Skarmeta, and M. Sánchez-Artigas, "Architecture and evaluation of a unified V2V and V2I communication system based on cellular networks," *Comput. Commun.*, vol. 31, no. 12, pp. 2850–2861, Jul. 2008.

Integration of Physical and Cognitive Human Models to Simulate Driving With a Secondary In-Vehicle Task

Helen J. A. Fuller, Matthew P. Reed, and Yili Liu, *Member, IEEE*

***Abstract*—Human behavior models give insight into people's choices and actions and are tools for predicting performance and improving interface design. Most models focus on a task's cognitive aspects or its physical requirements. This research addresses the divide between cognitive and physical models by combining two models to produce an integrated cognitive–physical human model that enables studying of complex human–machine interactions. The capabilities of the integrated model are evaluated in a task scenario with both cognitive and physical components, i.e., driving while performing a secondary in-vehicle task. When applied in this way, the integrated model is called the Virtual Driver model and can replicate basic driving, in-vehicle tasks, and resource-sharing behaviors, providing a new way to study driver distraction. The model has applicability to interface design and predicting staffing requirements and performance.**

***Index Terms*—Driver distraction, driver modeling, queuing network, secondary task.**

Manuscript received September 7, 2010; revised May 26, 2011 and September 5, 2011; accepted December 3, 2011. Date of publication February 3, 2012; date of current version May 30, 2012. This work was supported by the Automotive Research Center, which is a U.S. Army Center of Excellence for Modeling and Simulation of Ground Vehicles led by the University of Michigan and the University of Michigan Industry Affiliation Program for Human Factors in Transportation Safety. The Associate Editor for this paper was A. Amditis.

H. J. A. Fuller was with the Department of Biomedical Engineering, University of Michigan, Ann Arbor, MI 48109-2099 USA. He is now with Applied Safety and Ergonomics, Ann Arbor, MI 48108 USA (e-mail: hjaf@umich.edu).

M. P. Reed is with the University of Michigan Transportation Research Institute, Ann Arbor, MI 48109 USA (e-mail: mreed@umich.edu).

Y. Liu is with the Department of Industrial and Operations Engineering, University of Michigan, Ann Arbor, MI 48109 USA (e-mail: yililiu@umich.edu).

Color versions of one or more of the figures in this paper are available online at http://ieeexplore.ieee.org.

Digital Object Identifier 10.1109/TITS.2012.2182764